This article has been accepted for publication in IEEE Transactions on Power Systems. This is the author's version which has not been fully edited and content may change prior to final publication. Citation information: DOI 10.1109/TPWRS.2023.3262501

Ecological Robustness-Oriented Grid Network Design for Resilience Against Multiple Hazards

Hao Huang*, *Member, IEEE,* Zeyu Mao*, *Member, IEEE,* Varuneswara Panyam†, Astrid Layton†, Katherine R. Davis, *Senior Member, IEEE**

***Abstract*—Power systems are critical infrastructure for reliable and secure electric energy delivery. Incidents are increasing, as unexpected multiple hazards ranging from natural disasters to cyberattacks threaten the security and functionality of society. Inspired by resilient ecosystems, this paper presents a resilient network design approach with an ecological robustness ($\mathrm{R_{ECO}}$)-oriented optimization to improve power systems' ability to maintain a secure operating state throughout unknown hazards. The approach uses $\mathrm{R_{ECO}}$, a *surprisal*-based metric that captures key features of an ecosystem's resilient structure, as an objective to strategically design the electrical network. The approach enables solvability and practicality by introducing a stochastic-based candidate branch creation algorithm and a Taylor series expansion for relaxation of the $\mathrm{R_{ECO}}$ formulation. Finally, studies are conducted on the $\mathrm{R_{ECO}}$-oriented approach using the IEEE 24 Bus RTS and the ACTIVSg200 systems. Results demonstrate improvement of the system's reliability under multiple hazards, network properties of robust structure and equally distributed power flows, and survivability against cascading failures. From the analysis, we observe that a more redundant network structure with equally distributed power flows benefits its resilience.**

***Index Terms*—Power Networks Design; Ecological Robustness; Mixed-Integer Nonlinear Programming; Power System Reliability; Power System Resilience**

I. Introduction

Power systems deliver the electric energy that ensures the functionality of modern society. However, the infrastructure is aging and remains vulnerable to physical disturbances and natural disasters [1], such as the Winter Storm Uri in Texas in 2021. The integration of communication networks into critical infrastructure enables improved functionality but also increases the risk of cyber-originated and combined cyber-physical attacks to cause unexpected outages [2], [3]. The design of a *resilient* grid network is thus an essential foundation for its inherent abilities to withstand such hazards.

Resilience is a property of systems that represents their ability to recover from adverse conditions. From a regional transmission operator perspective, Chen *et al.* emphasize the necessity of constructing a robust grid to allow operators to address various contingencies on any given day [4]. In [5], Gholami *et al.* list different areas of resilience enhancement regarding system planning and operations, where long-term planning resilience enhancements lay the foundation for short-term operational resilience enhancements. Both [6], [7] find that redundant and robust network structures are effective for improving power system resilience under extreme conditions. These works highlight the importance of network design for enhancing power system resilience, while motivating the need to better understand and characterize the effective use of design against extreme events. Inspired by resilient ecosystems, this work develops a resilience-oriented design approach for large scale power systems that improves their inherently ability to absorb the disturbances from multiple hazards. The novelty of this work is to introduce an optimization based resilient design approach that is realistic, scalable, and extensible to translate the long-term resilient trait of ecosystems, ecological robustness ($\mathrm{R_{ECO}}$), into power network design with the consideration of power system constraints, including the power balance, power flow equations, and operational limits. The goal of the proposed *R_{ECO} Oriented Power Network Design Problem* is to strategically add redundancy to power networks and satisfy the constraints of power systems for improving the system's resilience. The main contributions of this paper are as follows:

- This paper presents a resilience-oriented approach to improve power systems' inherent ability to tolerate *unexpected* high-impact disturbances and maintain functionality securely. A quantitative resilience metric, $\mathrm{R_{ECO}}$, is formulated as an objective for network optimization considering the power system's constraints to guide resilient power network design, ahead-of-time without intelligence of the threat.
- A stochastic-based algorithm to create candidate branches and a Taylor Series Expansion of the logarithm function in the formulation are proposed to scalably solve the optimization, and the $\mathrm{R_{ECO}}$-oriented design problem is solved for 24- and 200-bus systems under different scenarios.
- The $\mathrm{R_{ECO}}$-oriented power networks are examined under different levels of *N-x* contingencies, and their network properties and power flow distributions are analyzed. The analyses show that a more redundant power network structure with more equally distributed power flows contributes to a more resilient power system.
- $\mathrm{R_{ECO}}$ is shown to be an effective metric to help measure and improve the inherent resilience of power networks. The formulation can guide design of power network structures considering power flows and ecosystems' resilient traits to achieve power systems' long-term resilience.

Section II reviews other resilient power network design approaches and introduces the research objective of this work. Section III presents related work on unexpected critical *multi-hazards* in power systems and the background of $\mathrm{R_{ECO}}$. Section IV introduces the proposed $\mathrm{R_{ECO}}$-oriented approach for improving power system resilience through resilient network design. Section V applies the R_{ECO}-oriented approach to a 24- and a 200-bus system, respectively. Section VI analyzes optimized networks regarding the system reliability under different levels of *N-x* contingencies and network properties. More discussions are in Section VII, and Section VIII concludes the paper.

II. Background and Research Objectives

Recently, several works have been proposed to optimally design and plan transmission and distribution systems to improve a system's resilience against natural disasters. In [8], Ma *et al.* present a two-stage stochastic mixed-integer linear program to optimally design the network with minimum investment and minimum expected loss of load during climate hazards. In [9], a framework is proposed to analyze the investment in power network enhancements with the evaluation of system resilience under natural disasters. In [10], a tri-level planning approach is proposed to expand and harden the coupled power distribution and transportation systems for improved resilience under random natural disasters with minimum investment. In [11], Garifi *et al.* propose a method to harden the power grid structure with minimum investment. The investment decision will improve the grid's recovery against natural disasters. All above works consider the adverse impact of natural disasters with stochastic models and formulate the resilient network design problem from the cost-effectiveness perspective. The improvement of resilience is observed and validated with less loss of load under the adverse scenarios. These works address resilience through different economic incentives for targeted hazards. However, there is a lack of an accepted and unified *resilience* objective that captures the inherent property of resilience considering the power network structure. By comparison, the research question addressed in this paper is *how to design a resilient power network structure that can enhance power systems' inherent ability to tolerate disturbances and maintain functionality securely regardless of the source of threats.* R_{ECO} captures the inherent property of resilience regarding the network design and power flow distribution, and it represents the inherent ability to absorb disturbances regardless of their sources or causes.

As presented in [12], *design, preparedness, and planning* have been recognized as the top three needs to enhance grid resilience; importantly, design and construction standards for higher performance are required. The research gap addressed in this paper is to integrate the property of resilience into power network design for enhanced inherent resiliency. This paper presents a resilience-driven approach for power network design with its inspiration from naturally resilient ecosystems. The proposed approach translates ecosystems' survivability and resilience traits to power grids under the guidance of a *quantitative* resilience objective.

The concept of *resilience* that we adopt dates back to the 1970s when *C.S. Holling* defined the *resilience* in ecology as "a measure of the ability to absorb changes of variables and parameters in systems [13]." Over millions of years' growth and development, ecosystems have survived from various *large-scale* and *unexpected* disturbances, showing the ability to absorb sudden changes in the system and maintain their state. This long-term resilience contributes to an ecosystem's unique network structure, and it results in a novel and practical benchmark for robust, sustainable, and resilient human networks design. This benchmark is quantified as ecological robustness (R_{ECO}) [14], [15] that adopts a *surprisal* model from *information theory* [16]. By modeling ecosystems as directional graph representations of energy transfer, the optimal R_{ECO} recognizes a balance of the pathway *efficiency* and *redundancy* in resilient ecosystems. Based on the similarity between ecosystems and power systems, [17], [18] introduce the potential of R_{ECO} to guide power network design for improved reliability. In [19], the authors propose a R_{ECO}-oriented optimal power flow to improve power systems' survivability against unexpected contingencies. All above works show the potential of applying R_{ECO} into power systems to improve resilience. However, the approach in [17] would not be practical to implement. For a 14-bus power grid, it is unrealistic to construct 80 branches to improve its resilience. Besides, [17], [18] are limited to small-scale power systems due to the mathematical formulation of the R_{ECO} and its optimization, while [19] only optimizes the power flow dispatch. Therefore, this paper introduces a comprehensive R_{ECO}-oriented resilient power network design approach that facilitates scalability and practicality for large-scale power systems.

Three challenges previously impeded the application of R_{ECO} for large-scale power network design. First, the nature of network design is a mixed-integer problem, which is a typical class of NP hard problem. With the increase of case size, the search domain expands exponentially, which adversely limits the efficiency for finding a global optimal. Second, the optimized networks in [17] directly connect buses in different voltage levels, which are impractical in power systems. Third, the formulation of R_{ECO} involves several layers of logarithm functions which need the input variables to be positive, namely the power flow direction needs to be the same during the solving process. However, power flow direction changes are prevalent in large-scale power systems, and it makes the mixed-integer nonlinear programming (MINLP) problem in [18] invalid for larger power systems. To deal with above challenges, this paper first introduces a stochastic based algorithm to create candidate branches with realistic electric parameters for large-scale power systems. It greatly reduces the search domain for the optimal structure and keeps the realism of the network structure. Then, we relax the formulation of R_{ECO} with a Taylor series expansion for the logarithm functions. The change of flow direction during the solving process will not cause the problem to be invalid. This improves the solvability and efficiency of the network design problem and ensures the practicality of the optimized resilient network design.

III. Related Work

A. Unexpected Multi-Hazard Scenarios

N-1 reliability is the basic requirement for modern power systems planning and operation [20]. However, the integration of communication networks and the increasing of system size expose power systems to more threats from both cyber and

This article has been accepted for publication in IEEE Transactions on Power Systems. This is the author's version which has not been fully edited and content may change prior to final publication. Citation information: DOI 10.1109/TPWRS.2023.3262501

physical domains. Thus, the abruptness of contingencies is increasingly harder to predict [21]. In [22], [23], authors have utilized Line Outage Distribution Factors (LODFs) and Group Betweenness Centrality (GBC) to identify sets of critical elements in large scale synthetic grids [24]. These sets of critical elements consist of multiple (3 to 8) branches across the *wide* area, which are statistically *unexpected* and can *adversely* disrupt power systems' operation and security. In [25], those *unexpected multi-hazards* have been achieved through Man-in-the-Middle attacks (*MiTM*) in a high fidelity cyber-physical power system testbed. Those incidents make the system experience operational stress, threatening grid security and resilience. The above *multi-hazard* scenarios provide a touchstone for measuring power system resilience against *unexpected* cyberattacks and natural disasters. Under *unexpected multi-hazards*, the system's inherent ability to absorb disturbances can be measured by its resulting operational violations as an indicator of its resilience.

B. Background of Ecological Robustness (R_{ECO})

Ulanowicz *et al.* and Fath *et al.* utilize a model of *surprisal* from *Information Theory* [16] to quantify the resilience of ecosystems as R_{ECO}. It considers the network structure and the transitions of energy and material among all species over the network [14], [15], [26]. Its formulation represents a given network's robustness as a function of its energy flow pathway's *redundancy* and *efficiency*.

Surprisal is defined with the following expression,

$$s_i = -k \times log(p_i) \tag{1}$$

where s_i is one's "surprisal" at observing an event *i* that occurs with probability p_i, and k is a positive scalar constant [27].

The *indeterminacy* (h_i) of an event i is then formulated as the product of the presence of an event p_i and its absence s_i:

$$h_i = -k \times p_i \times log(p_i) = s_i \times p_i \tag{2}$$

It measures how likely the event i will change for a given event i, if we know the probability of event i will occur ($p_i >> 0$) and the surprisal of event i that the system is doing something else most of the time ($s_i >> 0$). It can be interpreted as follows: for a given system, those low probability events can cause high impacts to the system, because they happen so rarely that the system doesn't expect; high probability events possess a low impact because they occur often and the system adapts to them [28].

With the above models of *surprisal* and *indeterminacy*, R_{ECO} is formulated with the following metrics.

The **Total System Throughput** (*TSTp*) is the sum of all flows within the system, which represents the system size [29],

$$TSTp = \sum_{i=1}^{N+3}\sum_{j=1}^{N+3} T_{ij} \tag{3}$$

where T_{ij} is the entry in *Ecological Flow Matrix* (*EFM*) [**T**]. Following the ecologists' modeling of food webs, the *EFM* is constructed with a system boundary. Fig 1 shows a hypothetical ecosystem and its conversion to [**T**]. The actors (species) that exchange energy based on a *prey-predator* relationship are within the system boundary, and the energy providers, energy consumers, and energy dissipation are placed outside of the system boundary [29]. Thus, [**T**] is a square $(N{+}3) \times (N{+}3)$ matrix containing flow magnitudes of transferred energy. N is the number of actors inside the system boundary, and the extra three rows/columns represent the system inputs, useful system exports, and dissipation or system exports [30]. It captures the energy interactions within and across the system boundary.

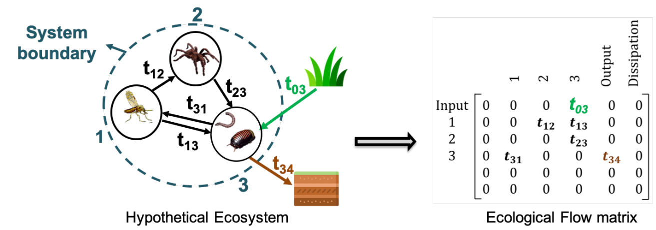

Fig. 1: The conversion of a hypothetical ecosystem into Ecological Flow Matrix. Replicated from [17].

The **Ascendency** (*ASC*) measures the scaled mutual constraint for system size and flow organization that describes the process of ecosystems' growth and development [31] with following expression,

$$ASC = -TSTp \times \sum_{i=1}^{N+3}\sum_{j=1}^{N+3}\left(\frac{T_{ij}}{TSTp} log_2\left(\frac{T_{ij}TSTp}{T_iT_j}\right)\right) \tag{4}$$

where $\frac{T_{ij}}{TSTp}$ is recognized as the probability of an event that interrupts T_{ij} with respect to all flows circulated in the system. $\frac{T_{ij}TSTp}{T_iT_j}$ measures the conditional probability of joint event i and j with knowledge of source node (*i*) and end node (*j*), where $T_i = \sum_{m=1}^{m=N+3} T_{im}$ and $T_j = \sum_{n=1}^{n=N+3} T_{nj}$. With the model of *indeterminacy* (Eqn. 2), the sum of $\frac{T_{ij}}{TSTp} log_2(\frac{T_{ij}TSTp}{T_iT_j})$ multiplies with *TSTp*, giving a dimensional version of network uncertainty. For the same size systems, a higher value of *ASC* means that a network has fewer options of pathways for flows moving from any one actor to another, resulting in a lower level of uncertainty.

The **Development Capacity** (*DC*) is the upper bound of *ASC* as the development and growth of ecosystems are limited [32],

$$DC = -TSTp \sum_{i=1}^{N+3}\sum_{j=1}^{N+3}\left(\frac{T_{ij}}{TSTp} log_2\left(\frac{T_{ij}}{TSTp}\right)\right) \tag{5}$$

Similar to *ASC*, *DC* is also the aggregate uncertainty, but without considering the source and end nodes. It captures the aggregated impacts (uncertainty) from all events (surprisals).

Then, R_{ECO} is then formulated as follows:

$$R_{ECO} = -\left(\frac{ASC}{DC}\right) ln\left(\frac{ASC}{DC}\right) \tag{6}$$

The ratio of *ASC* and *DC* reflects the *pathway efficiency* for a given network, while its natural logarithm shows the network's *pathway redundancy* [14]. Thus, R_{ECO} is a function of these two opposing but complementary attributes, where

This article has been accepted for publication in IEEE Transactions on Power Systems. This is the author's version which has not been fully edited and content may change prior to final publication. Citation information: DOI 10.1109/TPWRS.2023.3262501

their balance achieves the optimal $\mathrm{R_{ECO}}$ that directly affects a system's long-term survival [14]. Multi-element contingency analyses in systems controlled for optimal $\mathrm{R_{ECO}}$ [19] have shown the ability for $\mathrm{R_{ECO}}$ to account for the presence of unknown events, or interruptions, that can happen in the system.

IV. Ecological Robustness-Oriented Approach for Resilient Power Networks

Modeling a power system analogous to an ecosystem enables construction of [**T**] with real power flows which enables $\mathrm{R_{ECO}}$ optimization and analysis [17], [18]. The analogy adopted between power grids and food webs sets the food web *actors* as generators and buses, the *system inputs* as energy supplied to generators from outside the system boundaries, the *useful exports* as loads (demand), and the *dissipation* as real power losses. Fig 2 shows an exemplar [**T**] for a grid with n generators and m buses.

With [**T**] constructed from real power flows, *DC* estimates the aggregated impacts of all events as the maximum power flow changes that can happen in the system. *ASC* estimates the dependence between events, and $\mathrm{R_{ECO}}$ estimates the robustness of the system. Then, by including $\mathrm{R_{ECO}}$ as an objective to guide network design, the optimized networks can better inherently absorb disturbances while maintaining functionality securely, thus improving their resilience.

A. Mixed-Integer Optimization Model

The *R_{ECO}-Oriented Power Network Design Problem* is built upon the Transmission Network Expansion Planning (TNEP) problem and implemented using `PowerModels.jl` with the objective of achieving optimal R_{ECO}. The problem is formulated through Equation (7)-(17) with the direct current (DC) power flow model. The novelty of this model is integrating knowledge of this resilient property from ecosystems with the physics in power systems for resilient power network design.

Objective:

$$Max(R_{ECO}) \tag{7}$$

Subject to:

$$[\mathbf{T}] = f(P_{ij}, P_{gen_i}, P_{load_i}, \alpha_{ij})$$
$$= \begin{bmatrix} 0, & P_{gen_i}, & 0, & \dots & \dots & 0 \\ 0, & \dots & P_{gen_i}, & 0, & \dots & 0 \\ 0, & \dots & \dots & \dots & \dots & 0 \\ 0, & \dots & P_{ij}, & \dots & P_{load_i}, & 0 \\ 0, & \dots & \dots & \dots & \dots & 0 \\ 0, & \dots & \dots & \alpha_{ij}P_{ij}, & P_{load_i}, & 0 \\ 0, & \dots & \dots & \dots & \dots & 0 \end{bmatrix} \tag{8}$$

$$R_{ECO} = -\left(\frac{ASC}{DC}\right) ln\left(\frac{ASC}{DC}\right) \tag{9}$$

$$ASC = -TSTp \sum_{i=1}^{N+3}\sum_{j=1}^{N+3}\left(\frac{T_{ij}}{TSTp} log_2\left(\frac{T_{ij}TSTp}{T_i T_j}\right)\right) \tag{10}$$

$$DC = -TSTp \sum_{i=1}^{N+3}\sum_{j=1}^{N+3}\left(\frac{T_{ij}}{TSTp} log_2\left(\frac{T_{ij}}{TSTp}\right)\right) \tag{11}$$

$$TSTp = \sum_{i=1}^{N+3}\sum_{j=1}^{N+3} T_{ij} \tag{12}$$

$$P_{ij}^l \leqslant P_{ij} \leqslant P_{ij}^u \ (\forall (i,j) \in \mathcal{B} \cup \mathcal{NB}) \tag{13}$$

$$P_{gen_i}^l \leqslant P_{gen_i} \leqslant P_{gen_i}^u \ (\forall i \in \mathcal{G}) \tag{14}$$

$$P_{ij} = B_{ij}(\theta_i - \theta_j) \ (\forall (i,j) \in \mathcal{B}) \tag{15}$$

$$P_{ij} = \alpha_{ij} B_{ij}(\theta_i - \theta_j) \ (\forall (i,j) \in \mathcal{NB}) \tag{16}$$

$$P_i = P_{load_i} - P_{gen_i} = \sum_j P_{ij} \ (\forall j \in \mathcal{M}) \tag{17}$$

where $\mathcal{B}$ is the set of existing branches, $\mathcal{NB}$ is the set of candidates of new branches, $\mathcal{M}$ is the set of buses, and $\mathcal{G}$ is the set of generators; P_{ij}^l and P_{ij}^u are the lower and upper bound of branch limit, respectively; $P_{gen_i}^l$ and $P_{gen_i}^u$ are the lower and upper bound of generator output, respectively.

		Gen 1	. . .	Gen n	Bus 1	. . .	Bus m	Output	Dissipation
Input	0	P_{gen1}	. . .	P_{genn}	0	. . .	0	0	0
Gen 1	0	0	. . .	0	P_{gen1}	. . .	0	0	0
.	.	.	. . .	.	.	. . .	.	.	.
Gen n	0	0	. . .	0	0	0	P_{genn}	0	0
Bus 1	0	0	. . .	0	0	. . .	P_{1m}	$P_{load\ 1}$	$P_{loss\ 1}$
.	.	.	. . .	.	$P_{ne\ i1}$	. . .	.	.	.
.	.	.	. . .	.	.	P_{ij}	$P_{ne\ im}$	.	.
.	.	.	. . .	.	.	$P_{ne\ ij}$	.	.	.
Bus m	0	0	. . .	0	P_{m1}	. . .	0	$P_{load\ m}$	$P_{loss\ m}$
	0	0	. . .	0	0	. . .	0	0	0
	0	0	. . .	0	0	. . .	0	0	0

Fig. 2: An exemplar of *Ecological Flow Matrix* [**T**] for a grid with n generators and m buses. The entries of [**T**] are P_{gen_i}, P_{ij} and $P_{ne_{ij}}$, P_{load_i}, P_{loss_i}. The P_{gen_i} is the real power output from generator i, which locates at the input row and the flow between generator and corresponding bus. The generators are treated as lossless with no dissipation. The P_{load_i} and P_{loss_i} are the real power consumption and real power loss, respectively, at Bus i. The P_{ij} and $P_{ne_{ij}}$ are the real power flows on the corresponding existing branch and candidate branch, respectively. Entries with zero values mean there is no power flow interaction among buses and generators.

The TNEP problem is formulated as a mixed-integer optimization problem where each candidate branch has a binary decision variable α_{ij} for the candidate branch from bus i to bus j. The initial value of α_{ij} equals to zero if the corresponding branch does not exist in the original network. If α_{ij} after optimization equals one, the branch is built to reach a maximum $\mathrm{R_{ECO}}$.

The calculation of $\mathrm{R_{ECO}}$ depends on [**T**] as expressed in Eqn. 8 with generator real power output P_{gen_i} of each generator, real power flow P_{ij} and $P_{ne_{ij}}$ from existing branches and candidate branches, power consumption at each load P_{load_i},

This article has been accepted for publication in IEEE Transactions on Power Systems. This is the author's version which has not been fully edited and content may change prior to final publication. Citation information: DOI 10.1109/TPWRS.2023.3262501

and binary decision variables α_{ij} for candidate branches. Fig. 2 illustrates the detailed formulation of **[T]** using the above variables. Power flow dispatch (P_{ij} and $P_{ne_{ij}}$) depends on the real (P_i) and reactive power (Q_i) injection at each bus, bus voltage (voltage magnitude V_i, voltage angle θ_i), and the network structure (α_{ij}) [33]. In this formulation, a DC power flow model is used, so voltage magnitude V_i is one, reactive power Q_i and real power losses P_{loss_i} are zero. Therefore, the decision variables of the *R_{ECO}-Oriented Power Network Design Problem* include each generator's real power input P_{gen_i}, voltage angle θ_i of each bus, and the binary decision variable α_{ij} for candidate branches. In this way, the proposed R_{ECO}-oriented approach will optimize the network structure (α_{ij}) and power flow dispatch (P_{gen_i} and θ_i) to maximize R_{ECO}. Eqn. (9)-(12) are the calculation of R_{ECO} using **[T]** through several layers of logarithm functions. Eqn. (13)-(17) are the power flow constraints for operating limits and power balance. This MINLP problem is thus a nonlinear non-convex optimization problem.

B. Stochastic Based Candidate Branches Creation

In the proposed MINLP problem in Section IV-A, rather than considering all potential branches to build, a set of candidate branches is considered. This represents that in reality, the planners have some *a priori* information about new lines to consider. To represent the impact of the variability of such a set on the formulation and its solution, assuming here that we do not know and cannot control what lines they will choose, and to serve as a proxy for this set, we implement the hypothetical scenario where this set is chosen randomly. This selection mechanism can be considered as a worst case scenario, which is suitable to study, as the true planners may be able to choose a better set than a random selection. Hence, by demonstrating algorithm's effectiveness even when it is assumed that no information is given about the candidate branch locations, it shows the potential of the approach to be this good or better in reality. This introduces opportunity for future study. Since the test cases do not include a candidate branch set, Algorithm 1 is used, with suitable electric parameters for each branch based on the existing grid information. This fills the gap of the lacked information for candidate branches to expand power networks. Unlike [17], [34] that use heuristics or pre-screening methods to find an optimal network structure, Algorithm 1 is a stochastic approach to select candidate lines that supports direct inclusion of R_{ECO} with power system constraints to optimize power network structure for inherent resilience.

The input for Algorithm 1 is the bus and branch information of a given power network, including identifier information, voltage levels, and branches' electric parameters. Algorithm 1 first classifies the existing branches into different voltage levels. The normal distribution is then used to represent the real-valued random variables. Thus, we take branches' electric parameters, including series resistance (R), series reactance (X), and shunt conductance (C), and capacity (MVA limit), as real-valued random variables following the *normal distribution*. Based on the case information, Algorithm 1 generates *normal distributions* for different electric parameters

Algorithm 1 Stochastic Based Realistic Candidate Branches Selection and Creation

Input = All branches' information from the case, the total number of candidate branches (M)
Classify branches based on the voltage level
while The number of candidate branches $< M$ **do**
  for Each Voltage Level **do**
    Collect the branch information for all parameters
    for Each Parameter **do**
      Compute the *mean* (μ) and *variance* (σ^2)
      Generate a *Normal Distribution* ($\mathcal{N}(\mu, \sigma^2)$)
    end for
  end for
  Select the *from bus* and *to bus* at the same voltage level using a *Uniform Distribution* ($\mathcal{U}$(0, M))
  Insert the parameter for the candidate branch from the *Normal Distribution* ($\mathcal{N}(\mu, \sigma^2)$).
end while

of branches at each voltage level. Algorithm 1 takes a 40% confidence interval to create valid and different electric parameters of R, X, and C in per unit for candidate branches in our case studies. The candidate branches' capacity are twice the average capacity of existing cases' branches. From ecologists' perspective, power networks are more efficient than redundant. Each network has a corresponding value of R_{ECO}, and any new branch could contribute to the improvement of R_{ECO}. In selecting the initial candidate branches, we hypothesize that all network structures have *approximately* the same probability of being the most resilient network based on R_{ECO}; hence, all branches are assumed to have the same probability to be selected using the *uniform distribution*. Algorithm 1 will select *M* candidate branches from all possible branches with the *uniform distribution* to reduce the searching domain. With a specified number of candidate branches (*M*), the probability of selecting candidate branches is ($\frac{1}{M}$)

Additional information such as geographic location, cost, and government policies can further improve the realism for choosing candidate branches and validating the cost-effectiveness for the network construction. Such information can help stakeholders determine the candidate branches instead of using Algorithm 1. The material, electrical parameters, and construction cost of candidate branches can also then be practically and accurately estimated.

One potential issue that may arise when adding branches is the so-called Braess paradox where adding one or more roads can cause congestion and slow down the traffic [35]. A similar situation has been observed in power systems where added branches induced congestion in the system [36], [37]. The Braess paradox is avoided in the proposed R_{ECO}-oriented power network design in Section IV-A because the optimization model will reject the branches that can cause congestion in the system. The results and analyses from the case studies also show this.

C. Relaxation of the Ecological Robustness Formulation

The formulation of R_{ECO} involves with several layers of logarithm functions, whose hard constraint is that its inputs must remain positive during the solving process for the proposed optimization problem using state-of-art MINLP solvers. However, the inputs for calculating R_{ECO} are the power flows, and their directions can be reversed during the solving process. In [18], its formulation fails to capture the feasible space for even small scale power systems, since the inputs are not constantly positive for the logarithm functions during the solving process. This creates a problem for large cases, where flow direction changes are more prevalent during the solving process. A Taylor Series Expansion of the natural logarithm function is thus used here to relax the formulation of R_{ECO} to ensure the feasibility of the proposed R_{ECO}-oriented power network design problem.

Considering the domain for the expansion, this paper utilizes the following relaxation, with $x > 0$ [38]:

$$\begin{aligned} ln(x) &= 2\sum_{n=1}^{\infty}\frac{((x-1)/(x+1))^{(2n-1)}}{(2n-1)} \\ &= 2[\frac{(x-1)}{(x+1)}+\frac{1}{3}(\frac{(x-1)}{(x+1)})^3+\frac{1}{5}(\frac{(x-1)}{(x+1)})^5+...] \end{aligned} \tag{18}$$

The logarithm function has a base of 2 in Equations (5) and (4). Using a property of logarithm functions,

$$log_2(x) = \frac{ln(x)}{ln(2)} \tag{19}$$

the Taylor Series Expansion of $log_2(x)$ can be expanded:

$$log_2(x) = \frac{2}{ln(2)}[\frac{(x-1)}{(x+1)}+\frac{1}{3}(\frac{(x-1)}{(x+1)})^3+\frac{1}{5}(\frac{(x-1)}{(x+1)})^5+...] \tag{20}$$

By adapting the first order Taylor Series Expansion of Equations (18) and (20) into Equation (9) - (11), the formulation of R_{ECO} can keep valid even with flow direction changes during the optimization process. The above formulation requires the input x not equal to -1. The x for the logarithm function in Equations (9)-(11) are $\frac{ASC}{DC}$, $\frac{T_{ij}TSTp}{T_iT_j}$, and $\frac{T_{ij}}{TSTp}$, respectively. $\frac{ASC}{DC}$ and $\frac{T_{ij}}{TSTp}$ are guaranteed within (-1,1) and $\frac{T_{ij}TSTp}{T_iT_j}$ is not equal to -1 for power systems. Then, the relaxed R_{ECO} in the proposed approach can thus be solved with large power grid networks.

V. Case Studies

This section applies the R_{ECO}-oriented approach for two power system cases: the IEEE 24 Bus RTS [39] and the 200-bus synthetic grid from [24], to improve their inherent ability to tolerate disturbances and maintain functionality securely. Algorithm 1 created 50, 100, 150, and 200 candidate branches for each case, respectively. Each case has a unique set of candidate branches, and each set of candidate branches does not belong to the others. For example, the set with 100 candidate branches does not include the set with 50 candidate branches. These candidate branches constitute 2^{50}, 2^{100}, 2^{150}, and 2^{200} different network structures to find the optimal R_{ECO}-oriented structure through solving the proposed R_{ECO}-oriented design problem.

The candidate branches are selected with the highest voltage rating for each case, since the highest voltage transmission lines are the backbone of the system for power transfer. The proposed approach (Equation 7-17) not only solves the network structure (α_{ij}), it also solves the optimal power flow dispatch with an output vector of generator real power and bus voltage setpoints (P_{gen_i} and θ_i). The resultant network design is analyzed with both the optimized network structure and the optimized network structure with the output vector, respectively. Thus, there two *types* of optimized networks analyzed for each scenario under each case study. The naming convention used for each network follows the pattern of *Original Case Name-Number of Candidate Branches-Structure/Str-OPF*. For the *-Structure* cases, they are the optimized network structure with the selected branches (α_{ij}) from the solution to analyze the optimized resilient network structure under *original operating points*; while for the *-Str-OPF* cases, they are the optimized network structure with the operating points of each generator's output and bus voltage (α_{ij}, P_{gen_i} and θ_i). The detailed case information have been made publicly available at [40].

The solver for the MINLP problem uses *Ipopt* [41], *Juniper* [42], and *Cbc* [43]. Since the MINLP in Section IV-A is a nonlinear non-convex problem, the solver can only find the local optimal point. All the problems were solved using a laptop with a 2.4 GHz processor and 8 GB memory. The value of the **Optimal R_{ECO}** from the solver is 0.3431. It is the mathematical optimal value of R_{ECO} with the Taylor Series Expansion. The results in Table I and II show the **Achieved R_{ECO}**, the **Operational Cost**, the **Number of Added Branches**, the **Real Power Losses**, the **Reactive Power Losses**, and the **Computation Time** for the IEEE 24 Bus RTS system and ACTIVSg200 system, respectively. The **Achieved R_{ECO}** is based on the optimized network structure with/without the output vector of generator real power output and bus voltage after solving the power flows of optimized case with the alternative current (AC) power flow model. The **Operational Cost** is based on the marginal cost (C_i) \$/MWhr and generator's output (P_i) MW with Eq. (21), so the unit is \$/hr.

$$Cost = \sum_{i=1}^{\mathcal{G}} C_i(P_i) \tag{21}$$

A. IEEE 24 Bus Reliability Test System (RTS)

The IEEE 24 Bus Reliability Test System (RTS) [39] has 24 buses and 37 branches. With 24 buses, there are 276 links that can be selected as candidate branches to expand the network structure. Fig 3 shows the R_{ECO} optimized network for the IEEE 24 Bus RTS system with 50 candidate branches (2^{50} different network structures), and 21 branches are added after the optimization.

Table I shows the results of all four scenarios for the IEEE 24 Bus RTS cases. The results of **Achieved R_{ECO}** show that the optimized networks have a higher value of R_{ECO} than the original case, and the *-Str-OPF* networks have a higher value of R_{ECO} than the *-Structure* networks (except for the

This article has been accepted for publication in IEEE Transactions on Power Systems. This is the author's version which has not been fully edited and content may change prior to final publication. Citation information: DOI 10.1109/TPWRS.2023.3262501

100 candidate branch scenario). The value of optimized R_{ECO} is close to the 'Window of Vitality' (0.3469-0.3679), which is the unique range of R_{ECO} for the resilient ecosystems [44].

With more branches constructed, the system has fewer real power losses but more reactive power losses, and the apparent power losses (MVA) are increasing as shown in Table I (except IEEE 24 Bus RTS-200-Structure and -Str-OPF). However, the extra losses from the new branches do not incur extra operational cost. When we compared the *-Structure* cases to the original case, the operational cost is reduced. On the other hand, the operational cost of all *-Str-OPF* cases increases with a slightly higher R_{ECO} values (except IEEE 24 Bus RTS-100-Str-OPF). With the optimized output vectors, P_{gen_i} and θ_i, the generators are also more equally contributing to the power supply for improving the R_{ECO}. Some expensive generators are generating more power, while some cheaper generators are producing less. It shows that the operational cost will not change much if only the network structure is more robust. As mentioned in Section IV-B, each set of candidate branches is unique. With the increasing numbers of candidate branches, the number of added branches does not increase. The added redundancy does not necessarily depend on the number of candidate branches. This confirms that R_{ECO} can *strategically* construct the network structure and operate power systems to improve the system's resilience and maintain power system constraints.

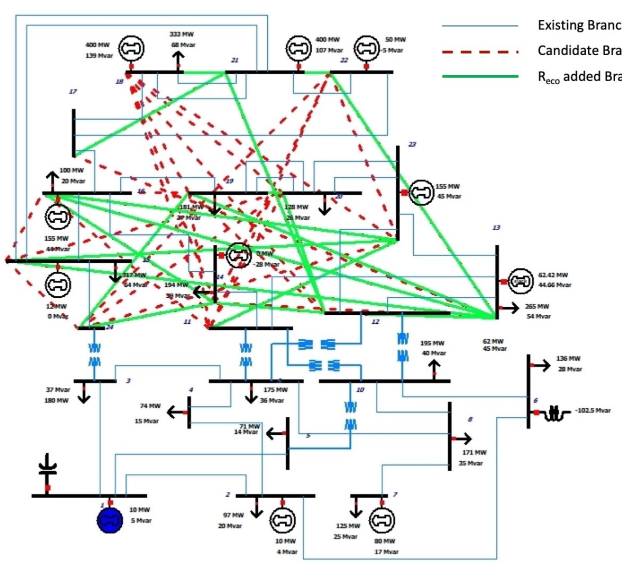

Fig. 3: R_{ECO}-oriented IEEE 24 Bus RTS network topology with 50 candidate branches (21 branches are constructed)

B. ACTIVSg200

The ACTIVSg200 case [45] has 200 buses and 246 branches. With 200 buses, there are 19900 links that can be selected as candidate branches, which contains 2^{19900} different network structures to be explored. Fig 4 shows the R_{ECO} optimized network for the ACTIVSg200 system with 50 candidate branches (2^{50} different network structures), and 26 branches are added after the optimization.

TABLE I: Results of R_{ECO}-Oriented Power Network Design for IEEE 24 Bus RTS

Use Case	Achieved R_{ECO}	Operational Cost ($/hr)	Number of Added Branches	Real Power Losses (MW)	Reactive Power Losses (MVar)	Computation Time (seconds)
IEEE 24 Bus RTS	0.3382	62263	0	51.22	650.27	0
IEEE 24 Bus RTS-50-Structure	0.3492	61061	21	29.91	789.69	1.74
IEEE 24 Bus RTS-50-Str-OPF	0.3496	78433	21	24.01	799.34	1.74
IEEE 24 Bus RTS-100-Structure	0.3514*	60716	25	19.92	891.52	8.54
IEEE 24 Bus RTS-100-Str-OPF	0.3502	71582	25	19.19	898.74	8.54
IEEE 24 Bus RTS-150-Structure	0.3454	60925	12	24.19	682.01	75.90
IEEE 24 Bus RTS-150-Str-OPF	0.3459	75525	12	22.39	691.87	75.90
IEEE 24 Bus RTS-200-Structure	0.3474	61432	8	34.40	598.75	23.02
IEEE 24 Bus RTS-200-Str-OPF	0.3479	78211	8	27.82	617.91	23.02

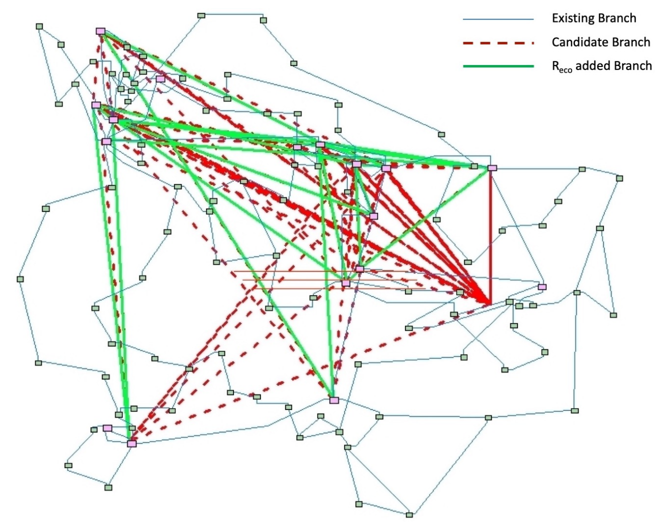

Fig. 4: R_{ECO}-oriented ACTVISg200 network topology with 50 candidate branches (26 branches are constructed)

TABLE II: Results of R_{ECO}-Oriented Power Network Design for ACTIVSg200

Use Case	Achieved R_{ECO}	Operational Cost ($/hr)	Number of Added Branches	Real Power Losses (MW)	Reactive Power Losses (MVar)	Computation Time (seconds)
ACTIVSg200	0.2510	49000	0	24.77	435.64	0
ACTIVSg200-50-Structure	0.2651	48909	26	19.21	598.83	58.64
ACTIVSg200-50-Str-OPF	0.2655	49725	26	18.04	593.64	58.64
ACTIVSg200-100-Structure	0.2578	51264	15	20.92	523.41	35.46
ACTIVSg200-100-Str-OPF	0.2599	51264	15	21.55	526.00	35.46
ACTIVSg200-150-Structure	0.2531	48923	5	22.23	471.84	84.09
ACTIVSg200-150-Str-OPF	0.2557	50044	5	22.73	470.65	84.09
ACTIVSg200-200-Structure	0.2671	52104	51	17.63	748.15	45.80
ACTIVSg200-200-Str-OPF	0.2708*	52014	51	16.75	764.93	45.80

All four scenarios are successfully solved and the results are shown in Table II. Compared to the IEEE 24 Bus RTS, the **Achieved R_{ECO}** values are much smaller in ACTIVSg200 cases. The original synthetic power grids are highly close to the real U.S power grids, which are quite sparse and efficient. Considering there are 2^{19900} different structures that can be explored, the created candidate branches may not have the *exact* optimal structure. Thus, the R_{ECO} for this synthetic grid is not improved as much as the IEEE 24 Bus RTS system.

For the ACTIVSg200 cases, all *-Str-OPF* networks have higher R_{ECO} than their corresponding *-Structure* networks. The new built branches incur extra whole power losses. Similar to the IEEE 24 RTS case, the real power losses also decrease while the reactive power losses increase. The operational cost of the ACTIVSg200-50-Structure and ACTIVSg200-150-Structure cases are less than the original operational cost even though there are extra branches and losses. The operational cost of other R_{ECO}-oriented cases increase slightly compared to the original case. The number of built branches does not increase with the increasing of candidate branches. This also demonstrates the R_{ECO} is *strategically* constructing the network structure and operating power systems.

VI. Network Analyses

The optimized networks are analyzed and compared with their original network for their reliability under *multi-hazard* scenarios and network properties regarding their structure and power flow distribution. All analyses are performed using AC power flow model.

A. Network Reliability Analysis

The *multi-hazard* contingencies are applied as different levels of *N-x* contingencies for each case. For *x=1*, they are planned contingencies; for *x>1*, they are *unexpected* contingencies. Under the contingencies, if there is one branch's power flow is over the limit or the voltage magnitude is out of the required limit, it is counted as **one** violation. If the power flow cannot be solved, then the contingency is marked as **unsolved**.

As for different case studies, the generation of N-*x* contingencies are different since the IEEE 24 Bus RTS system is relatively small compared with the ACTIVSg200 system. For the IEEE 24 Bus RTS cases, comprehensive *N-1*, *N-2* and *N-3* contingency analyses are performed for all power system components, including branch, bus and generator. The loss of any bus can cause more elements to be disconnected simultaneously. Thus, the *N-3 bus* contingencies can cause multiple components (generators and branches) disconnected. This can have a similar impact on generator unavailability like the Texas Winter Storm [46]. For the ACTIVSg200 cases, a comprehensive *N-2* and *N-3* contingency analysis is difficult to complete, due to the large number of components. The *N-1* contingency analysis is done for the branch, bus, and substations, respectively. Since all generators in ACTIVSg200 case are connected through transformers, the *N-1* branch contingencies include all *N-1* generator contingencies. The loss of one bus and one substation can catastrophically impact the entire system with multiple components (*N-x*) disconnected. It provides validation of the redesigned system's ability to tolerate disturbances and maintain functionality securely. For the ACTIVSg200 cases, the *unexpected* critical *multi-hazard* contingencies from [22], [23] are also considered. As mentioned in Section III-A, such critical *N-x* contingencies (*x* ranges from 3 to 8) are selected through LODFs and GBC as multiple branches widely spread in the system, whose loss may cause catastrophic impact to the system. Such critical contingencies are both geographically wide spread and statistically rare, which make them a touchstone to study resilience in large-scale systems. All the contingency analyses investigated here are performed without remedial actions. The basic control mechanism, such as automatic generation control (AGC) and automatic voltage regulator (AVR), are retained at their original settings. This provides a fair study about each system's inherent ability to tolerate unexpected *multi-hazard* disturbances and maintain functionality securely, thus justifying the improvement of resilience.

With more branches built after the optimization, there are more *N-1*, *N-2* and *N-3* contingencies than the original case, especially for the IEEE 24 Bus RTS case. To fairly compare the reliability, we then normalize the number of violations with the total number of *N-x* contingencies. Fig. 5 shows the normalized violations (total violations/total number of contingencies), and Fig. 6 shows the unsolved *N-2* and *N-3* contingencies for all variations of the IEEE 24 Bus RTS cases. Overall, the R_{ECO}-oriented network structure and operation schemes are more reliable than the original case with far fewer normalized violations and unsolved contingencies. With the proposed R_{ECO}-oriented approach, the *unsolved N-2* contingencies are completely resolved and the number of *unsolved N-3* contingencies reduced from 148 to less than 20. This ensures the observability of the system during disturbances and shows an outstanding improvement of resilience. The IEEE 24 Bus RTS-100-OPF case has the best performance among all cases. Even though its achieved R_{ECO} is smaller than the corresponding *-Structure* case, they have the same network structure. The redundant network structure contributes to the improved resilience.

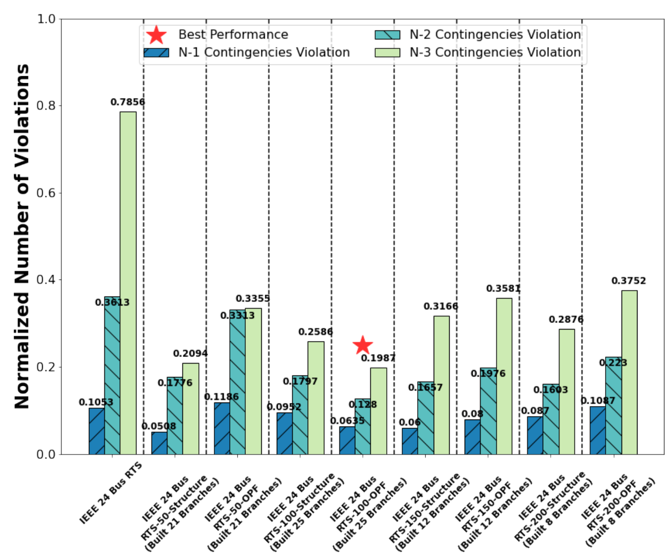

Fig. 5: Normalized Violations Comparison of R_{ECO}-Oriented Power Network for all variations of IEEE 24 Bus RTS cases (Table I)

Fig 7 shows the contingency analysis for all ACTIVSg200 cases. Overall, the R_{ECO}-oriented networks are much more resilient than the original network. All the optimized ACTIVSg200 cases maintain the same *N-1 branch* reliability as the original network. Under the *N-1* Bus, *N-1* Substation contingencies, and *unexpected* multi-hazard contingencies, all

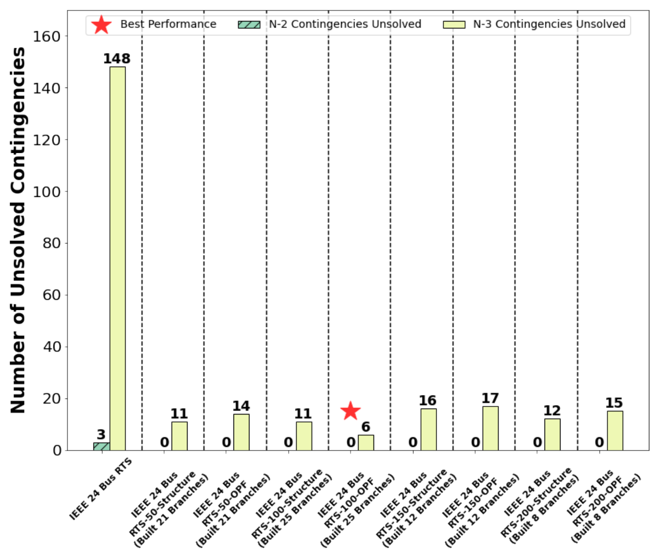

Fig. 6: Unsolved Contingencies Comparison of R_{ECO}-Oriented Power Network for all variations of IEEE 24 Bus RTS cases (Table I)

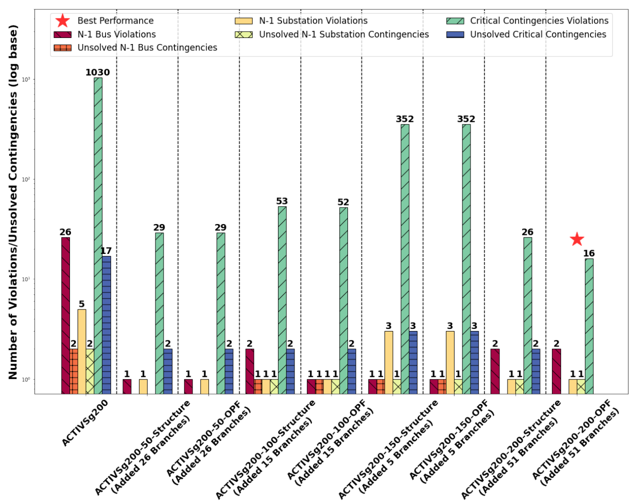

Fig. 7: Reliability Comparison of R_{ECO}-Oriented Power Network for all variations of ACTIVSg200 cases (Table II)

the R_{ECO}-oriented networks are *more* reliable with much fewer violations and unsolved situations. The ACTIVSg200-200-OPF has the best performance out of all the optimized networks with minimum violations and unsolved contingencies with the highest achieved R_{ECO}.

B. Network Properties Analysis

An entropy based network robustness metric (R_{CF}) is used to identify cascading failures in power systems [47]. The analysis of R_{CF} can capture how likely it is for the network to experience cascading failures. With a higher value of R_{CF}, the network is more robust and less likely to have a cascading failure [47]. The calculation of R_{CF} follows,

$$R_{CF} = \sum_{i=1}^{N} R_{n,i}\delta_i \tag{22}$$

$$R_{n,i} = -\sum_{i=1}^{L} \alpha_i p_i log(p_i) \;\; and \;\; \delta_i = \frac{P_i}{\sum_{j=1}^{N} P_j} \tag{23}$$

where α_i is the ratio between the maximum capacity and the load of corresponding line i; p_i is the normalized flow values on the out-going links; P_i is the total power distributed by node i and N is the number of nodes in the network.

All network structures are analyzed for typical complex network properties, including the average node degree ($\bar{d}$), clustering coefficient ($\bar{c}$), average betweenness centrality measures ($\bar{b}$) and average shortest path ($\bar{l}$) [48],

$$\bar{d} = \frac{\sum e}{\sum n} \; ; \quad \bar{c} = \frac{\sum_i \frac{\sum_{j,k} A_{ij}A_{jk}A_{ki}}{\sum_j A_{ij}(\sum_j A_{ij}-1)}}{\sum n} \; ; \tag{24}$$

$$\bar{l} = \frac{\sum_{i,j} dist(v_i, v_j)}{\sum i, jhas\_path(v_i, v_j)} \; ; \quad \bar{b} = \sum_{s,t\in V} \frac{\sigma(s,t|e)}{\sigma(s,t)} \tag{25}$$

where e is the edge and n is the node in graph; $\sum n$ is the total number of nodes in the graph; A is the adjacency matrix of the graph; $\sigma(s,t)$ represents the number of shortest paths in the graph between s and t; $\sigma(s,t|e)$ is the number of shortest paths in the graph between s and t that contain edge e.

The power flow distribution is also investigated by calculating the *Mean* and *Standard Deviation (STD)* of all branches' real power flow (pf), reactive power flow (rf), and the line percentage of MVA limit (MVA%) using Eqn. (26). For the power flow, the x_i are all branches' pf and rf, respectively. For the line percentage, the x_i are all branches' MVA%. The N is the total number of branches.

$$\overline{x} = \frac{1}{N}\sum_{i=i}^{n} x_i \; ; \quad s(x) = \sqrt{\frac{1}{N-1}\sum_{i=1}^{N}(x_i - \overline{x})^2} \tag{26}$$

Table III shows the network properties for all network structures and the corresponding optimal power flow. The R_{ECO}-oriented networks have better network properties than their original counterparts. All the R_{ECO}-oriented networks have higher R_{CF}, showing that the R_{ECO} corresponds to an improved R_{CF} against cascading failures. Increasing R_{CF} is found to highly correlate with increasing R_{ECO}, except the optimized results of the IEEE 24 Bus RTS with 100 candidate branches. Although formulations of both R_{ECO} and R_{CF} are based on an entropy model, their modeling details are different. R_{CF} is based on branch flow limits, while R_{ECO} is based on network structure, flow magnitudes, and flow directions. There can be some discrepancies between these two metrics.

All the R_{ECO}-oriented networks have larger $\bar{d}$ and $\bar{c}$, and reduced $\bar{b}$ and $\bar{l}$. It shows these networks are more robust, reducing the significance of nodes (buses) and paths (branches) in the system, which spreads out the system's risks, from both perspectives of severity and probability. For actual networks, the $\bar{d}$ is in the range of (2.58, 2.61), the $\bar{c}$ is in the range of (0.032, 0.058), the $\bar{b}$ is in the range of (0.083, 0.40), and the $\bar{l}$ is in the range of (14.2, 29.2) [45]. The results show that the optimized ACTIVSg200 networks' $\bar{d}$ and $\bar{c}$ are close to the actual systems, but the $\bar{b}$ and $\bar{l}$ are not. These can be explained by the way candidate branches were selected at their highest voltage level for each case, whose distance is shorter than branches between different voltage levels.

The *Mean* and *STD* of all the branches' real power flow (pf), reactive power flow (rf), and line percentage of MVA limits (MVA%) show that the $\mathrm{R_{ECO}}$-oriented networks distribute power flow more equally than the original network with reduced values in those measures. The Mean (pf) and STD (pf) in each *-Str-OPF* network are smaller than the *-Structure* network showing a more equally distributed real power flows, while the *-Structure* networks more equally distribute reactive power flows than *-Str-OPF* networks with smaller value of Mean (rf) and STD (rf). These facts could explain that even though the real power flows of the *IEEE 24 Bus RTS-150-Str-OPF* are more equally distributed than *IEEE 24 Bus RTS-150-Structure*, its $\mathrm{R_{CF}}$ is smaller. The α_i for $\mathrm{R_{CF}}$ (Eqn. 23) is the ratio between maximum line capacity considering real and reactive power, while the line loading in its calculation is only real power. With less equally distributed reactive power, its $\mathrm{R_{CF}}$ can be reduced. Similarly, since [**T**] and $\mathrm{R_{ECO}}$ only consider the real power flows, the reactive power flows can be distributed less equally to support the new built branches. Thus, the *-Str-OPF* cases may less equally distribute the power flows regarding the loading capacity, with higher value of the Mean (MVA%) and STD (MVA%) than the corresponding *-Structure* cases. In the optimized network, the reduced STD (pf), STD (rf), and STD (MVA%), compared to their original distributions, show that the power flows are closer to each other, and the newly built branches do not cause power flow increases on other branches. This also shows the proposed approach does not cause Braess paradox.

VII. Discussion

The proposed *R_{ECO} oriented approach for resilient power networks* is a typical NP-hard problem. Although the cases are different, the total number of topologies that the proposed approach explored is the same, which are 2^{50}, 2^{100}, 2^{150}, and 2^{200}. With the case size increasing, the computation time increases from 1.7 seconds to 84.09 seconds because of more power system variables (P_i and θ_i) and more complicated network structures. Thus, the computation time and complexity of the proposed approach depend on the number of power system variables and network structure.

Unlike a traditional network expansion problem using the AC power flow model [49], [50], [34], this paper does not consider auxiliary equipment for new branches in the formulation. The proposed $\mathrm{R_{ECO}}$-oriented power network design problem is based on the DC power flow model. The optimized network's reliability and network properties are then analyzed through solving the AC power flow model. From the analyses, the optimized power network structures with more equally distributed power flows have a greatly improved inherent ability to tolerate disturbances and maintain functionality securely. The improved resilience is shown by fewer operational violations and unsolved contingencies under the conventional *N-1* and unexpected *multi-hazard* contingencies. The candidate branches are created in Algorithm 1 without construction cost data. Thus, we are not able to perform as detailed a cost effectiveness analysis as in [8], [9], [10], [11].

Fig 8 shows the comparison of $\mathrm{R_{ECO}}$ for eight power grids and a set of 38 food webs. The smaller power grids (5- to 14-bus cases) are optimized by a heuristic method in [17] and the larger power grids are optimized by the proposed approach in this paper. The $\mathrm{R_{ECO}}$ of the food webs fall into the range of 'Window of Vitality', while the $\mathrm{R_{ECO}}$ of the original power grids fall outside this range, especially the large and sparsely-connected power grids. After the network optimization, their $\mathrm{R_{ECO}}$ is improved, as well as their inherent ability to absorb disturbances. However, the $\mathrm{R_{ECO}}$ is not within the 'Window of Vitality' for the cases in this paper. Two possible reasons for this are: (1) the desired 'Window of Vitality' values may be different for power systems compared to food webs, and (2) the sets of candidate branches do not include *all* network structures, so it is possible that the solution is not the *exact* optimal structure recognized by $\mathrm{R_{ECO}}$. Compared to the heuristic method in [17] whose optimized cases are within 'Window of Vitality,' the proposed approach in this paper is more realistic with far fewer branches built. The approach in [17] is limited to a 14-bus system, thus we cannot directly compare both methods. The 14-bus case constructs 60 branches in [17] with a global heuristic search, while the proposed approach builds 51 branches for the ACTIVSg200 case. It shows that the proposed $\mathrm{R_{ECO}}$-oriented approach with power flow constraints and limited search domain can realistically and strategically guide the power network design. Although the added branches slightly increase the operational cost for some scenarios, the improvement of reliability under different levels of *N-x* contingencies and their network properties justifies this increased cost. In [19], $\mathrm{R_{ECO}}$ was used to optimize the power flow distribution. This paper uses $\mathrm{R_{ECO}}$ to guide the power network design to further enhance its inherent capability to tolerate disturbances and maintain functionality securely. By strategically adding branches, the $\mathrm{R_{ECO}}$-oriented power networks are more resilient and survivable against multi-hazard contingencies, with much fewer violations and unsolved contingencies. From Table I, Figure 5 and 6, the optimal $\mathrm{R_{ECO}}$-oriented IEEE 24 Bus RTS system reduces 70% violations and 96% unsolved contingencies with 25 added branches. From Table II and Figure 7 the optimal $\mathrm{R_{ECO}}$-oriented ACTIVSg200 case reduces 98% violations and unsolved contingencies with 51 added branches. This level of resilience enhancement was not achieved in [19]. It shows that $\mathrm{R_{ECO}}$ can be an *accepted and unified* metric that captures power networks' inherent property of resilience.

The correlation among $\mathrm{R_{ECO}}$, R_{CF}, complex network properties and power flow distribution shows that the $\mathrm{R_{ECO}}$-oriented power network structure is more resilient against *multi-hazard* and cascading failures due to the redundant network structure with equally distributed power flows. It is worth noting that the reactive power losses are predominant in transmission network as observed in Table I and II. With more branches built, the optimized systems have more reactive power losses. There should be some auxiliary equipment along with the new branches for reactive power compensation as in [34]. However, to investigate the influence of network structure to resilience,

This article has been accepted for publication in IEEE Transactions on Power Systems. This is the author's version which has not been fully edited and content may change prior to final publication. Citation information: DOI 10.1109/TPWRS.2023.3262501

TABLE III: Network properties for all variations of the IEEE 24 Bus RTS and ACTIVSg200 systems.

Use Case	Achieved R_{ECO}	R_{CF}[47]	$\bar{d}$	$\bar{c}$	$\bar{b}$	$\bar{l}$	Mean(pf)	STD(pf)	Mean(rf)	STD(rf)	Mean(MVA%)	STD(MVA%)
IEEE 24 Bus RTS	0.3382	1.121	2.833	0.03472	0.10063	3.2138	117.19	86.83	27.95	23.52	32.35	19.04
IEEE 24 Bus RTS-50-Structure	0.3492	3.328	4	0.17698	0.07246	2.5942	67.01	53.33	19.79	19.31	19.54	16.35
IEEE 24 Bus RTS-50-Str-OPF	0.3496	3.413	4	0.17698	0.07246	2.5942	62.94	51.00	21.46	19.86	18.93	16.11
IEEE 24 Bus RTS-100-Structure	0.3514	4.009	4.333	0.175	0.06637	2.4601	56.34	43.71	18.91	19.02	17.02	15.97
IEEE 24 Bus RTS-100-Str-OPF ⋆	0.3502	4.043	4.333	0.175	0.06637	2.4601	51.47	42.57	19.57	19.67	16.48	17.22
IEEE 24 Bus RTS-150-Structure	0.3454	2.758	3.5	0.09861	0.08037	2.7681	69.68	60.11	20.32	22.60	21.24	18.22
IEEE 24 Bus RTS-150-Str-OPF	0.3459	2.495	3.5	0.09861	0.08037	2.7681	68.54	57.76	21.37	23.28	21.13	18.1
IEEE 24 Bus RTS-200-Structure	0.3474	1.979	3.417	0.11389	0.07790	2.7138	97.94	60.66	25.19	22.69	26.94	16.36
IEEE 24 Bus RTS-200-Str-OPF	0.3479	2.094	3.417	0.11389	0.07790	2.7138	88.79	52.59	24.74	24.22	25.13	15.72
ACTIVSg200	0.2510	1.565	2.46	0.03723	0.03531	7.9913	37.54	56.65	7.70	9.95	18.01	19.06
ACTIVSg200-50-Structure	0.2651	2.785	2.65	0.04399	0.02899	6.7396	34.00	51.06	5.94	7.28	16.11	18.19
ACTIVSg200-50-Str-OPF	0.2655	2.802	2.65	0.04399	0.02899	6.7396	33.18	50.61	5.96	7.27	15.57	17.30
ACTIVSg200-100-Structure	0.2578	2.204	2.55	0.03751	0.03061	7.0597	35.25	53.02	6.52	8.31	16.80	18.41
ACTIVSg200-100-Str-OPF	0.2599	2.168	2.55	0.03751	0.03061	7.0597	35.54	54.36	6.89	8.89	16.24	16.85
ACTIVSg200-150-Structure	0.2531	1.706	2.51	0.03654	0.03145	7.2272	36.90	55.29	7.18	8.95	17.59	18.78
ACTIVSg200-150-Str-OPF	0.2557	1.704	2.51	0.03654	0.03145	7.2272	37.48	58.73	7.51	9.40	16.91	16.94
ACTIVSg200-200-Structure	0.2671	4.207	2.82	0.05346	0.02787	6.5181	30.50	48.63	5.10	6.55	14.61	17.89
ACTIVSg200-200-Str-OPF ⋆	0.2708	4.207	2.82	0.05346	0.02787	6.5181	30.50	48.63	5.22	6.69	14.02	16.36

[1] ⋆: Best reliability.

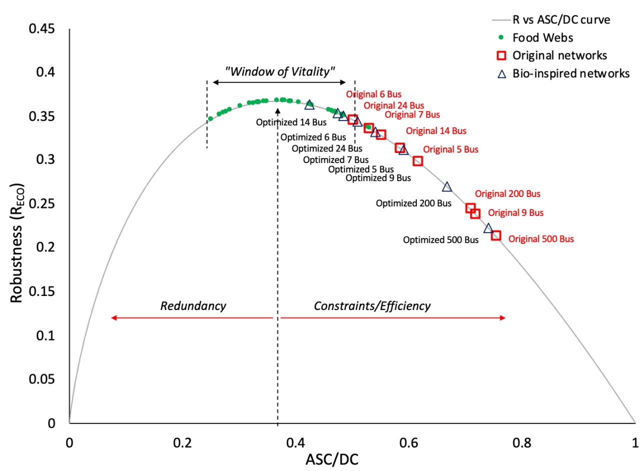

Fig. 8: $\mathrm{R_{ECO}}$ curve for eight power grids and their $\mathrm{R_{ECO}}$-oriented versions, as well as a set of 38 food webs (Data source: [17]).

all systems keep their original real and reactive power capacity. Thus, the improvement of resilience solely comes from the $\mathrm{R_{ECO}}$-oriented network structure. With extra auxiliary devices for reactive power support, the optimized systems can be more reliable and resilient under the contingencies. All above analyses demonstrate the effectiveness of using $\mathrm{R_{ECO}}$ as a *guidance* to *strategically* design and operate power grids to improve its ability to absorb sudden and big disturbances in the system while maintaining their functions securely, thereby enhancing their resilience.

VIII. Conclusion

This work addresses a power system's need to withstand distributed threats arising from natural, accidental, and intentional causes that can create multi-hazard scenarios of x elements across a wide area with severe impact. To achieve this, a power system resilient design approach is presented, inspired from long-term resilient ecosystems. The resilience-oriented power grid network design problem is formulated and solved, with the goal to improve power systems' inherent ability to tolerate disturbances and maintain functionality securely. The $\mathrm{R_{ECO}}$-oriented power networks are analyzed under *N-x* contingencies, network properties, and operational cost. Results show the $\mathrm{R_{ECO}}$-oriented networks have fewer operational violations and unsolved contingencies with more redundant network structure and more equally distributed power flows. The $\mathrm{R_{ECO}}$-oriented optimization is generalizable as a resilient network design approach that improves a network's ability to withstand unknown threats.

Future work can extend upon this methodology from the following two aspects. On the one hand, the impact of reactive power for the calculation and optimization of $\mathrm{R_{ECO}}$ in power networks can be investigated for reactive power planning for better resiliency. On the other hand, the economic factors, such as construction fee, electricity price, and penalty of unserved load, can be integrated with the proposed model to better understand the trade-offs between inherent resiliency and economics. Further, the projection of load growth and renewable energies integration can be taken into consideration for *future* resilient and economic power network design.

Acknowledgment

The authors would like to acknowledge the Texas A&M Energy Institute, the National Science Foundation under awards 1916142 and 2220347, and the US Department of Energy Cybersecurity for Energy Delivery Systems program under award DE-OE0000895 for their support of this work.

References

[1] S. A. Shield, S. M. Quiring, J. V. Pino, and K. Buckstaff, "Major impacts of weather events on the electrical power delivery system in the united states," *Energy*, vol. 218, p. 119434, 2021.

[2] E. Targett. (2020, March) High Voltage Attack: EU's Power Grid Organisation Hit by Hackers. [Online]. Available: https://www.cbronline.com/news/eu-power-grid-organisation-hacked

[3] Defense Use Case, "Analysis of the cyber attack on the ukrainian power grid," *Electricity Information Sharing and Analysis Center (E-ISAC)*, 2016.

[4] H. Chen, F. S. Bresler III, M. E. Bryson, K. Seiler, and J. Monken, "Toward bulk power system resilience: approaches for regional transmission operators," *IEEE Power and Energy Magazine*, vol. 18, no. 4, pp. 20–30, 2020.
[5] A. Gholami, T. Shekari, M. H. Amirioun, F. Aminifar, M. H. Amini, and A. Sargolzaei, "Toward a consensus on the definition and taxonomy of power system resilience," *IEEE Access*, vol. 6, pp. 32 035–32 053, 2018.
[6] M. Panteli, P. Mancarella, D. N. Trakas, E. Kyriakides, and N. D. Hatziargyriou, "Metrics and quantification of operational and infrastructure resilience in power systems," *IEEE Transactions on Power Systems*, vol. 32, no. 6, pp. 4732–4742, 2017.
[7] M. Panteli and P. Mancarella, "Modeling and evaluating the resilience of critical electrical power infrastructure to extreme weather events," *IEEE Systems Journal*, vol. 11, no. 3, pp. 1733–1742, 2015.
[8] S. Ma, S. Li, Z. Wang, and F. Qiu, "Resilience-oriented design of distribution systems," *IEEE Transactions on Power Systems*, vol. 34, no. 4, pp. 2880–2891, 2019.
[9] T. Lagos, R. Moreno, A. N. Espinosa, M. Panteli, R. Sacaan, F. Ordonez, H. Rudnick, and P. Mancarella, "Identifying optimal portfolios of resilient network investments against natural hazards, with applications to earthquakes," *IEEE Transactions on Power Systems*, vol. 35, no. 2, pp. 1411–1421, 2019.
[10] M. Shahidehpour, W. Gan, W. Yao, J. Wen, J. Guo, A. Paaso, S. Pandey, and A. Vukojevic, "A tri-level planning approach to resilient expansion and hardening of coupled power distribution and transportation systems," *IEEE Transactions on Power Systems*, 2021.
[11] K. Garifi, E. S. Johnson, B. Arguello, and B. J. Pierre, "Transmission grid resiliency investment optimization model with socp recovery planning," *IEEE Transactions on Power Systems*, vol. 37, no. 1, pp. 26–37, 2021.
[12] D. T. Ton and W. P. Wang, "A more resilient grid: The us department of energy joins with stakeholders in an r&d plan," *IEEE Power and Energy Magazine*, vol. 13, no. 3, pp. 26–34, 2015.
[13] C. S. Holling, "Resilience and stability of ecological systems," *Annual review of Ecology and Systematics*, vol. 4, no. 1, pp. 1–23, 1973.
[14] R. E. Ulanowicz, S. J. Goerner, B. Lietaer, and R. Gomez, "Quantifying sustainability: resilience, efficiency and the return of information theory," *Ecological Complexity*, vol. 6, no. 1, pp. 27–36, 2009.
[15] R. E. Ulanowicz, "Quantitative methods for ecological network analysis," *Computational Biology and Chemistry*, vol. 28, no. 5, pp. 321–339, 2004.
[16] R. M. Gray, *Entropy and information theory*. Springer Science & Business Media, 2011.
[17] V. Panyam, H. Huang, K. Davis, and A. Layton, "Bio-inspired design for robust power grid networks," *Applied Energy*, vol. 251, p. 113349, 2019.
[18] H. Huang, V. Panyam, M. R. Narimani, A. Layton, and K. R. Davis, "Mixed-integer optimization for bio-inspired robust power network design," in *52nd North American Power Symposium*, 2021, Conference Proceedings.
[19] H. Huang, Z. Mao, A. Layton, and K. R. Davis, "An ecological robustness oriented optimal power flow for power systems' survivability," *IEEE Transactions on Power Systems*, vol. 38, no. 1, pp. 447–462, 2023.
[20] L. Chuck, E. Luke, D. Michael, K. David, T. Mark, and G. Wayne, "Transmission system planning performance requirements," North American Electric Reliability Corporation (NERC), Application Guide, 2015. [Online]. Available: https://www.nerc.com/pa/Stand/Pages/AllReliabilityStandards.aspx?jurisdiction=United%20States
[21] S. Pahwa, C. Scoglio, and A. Scala, "Abruptness of cascade failures in power grids," *Scientific Reports*, vol. 4, no. 1, pp. 1–9, 2014.
[22] M. R. Narimani, H. Huang, A. Umunnakwe, Z. Mao, A. Sahu, S. Zonouz, and K. Davis, "Generalized contingency analysis based on graph theory and line outage distribution factor," *IEEE Systems Journal*, vol. 16, no. 1, pp. 626–636, 2021.
[23] H. Huang, Z. Mao, M. R. Narimani, and K. R. Davis, "Toward efficient wide-area identification of multiple element contingencies in power systems," in *2021 IEEE Power & Energy Society Innovative Smart Grid Technologies Conference (ISGT)*. IEEE, 2021, pp. 01–05.
[24] A. Birchfield, "Electric grid test case repository," Texas A&M University, College of Engineering. [Online]. Available: https://electricgrids.engr.tamu.edu/
[25] A. Sahu, P. Wlazlo, Z. Mao, H. Huang, A. Goulart, K. Davis, and S. Zonouz, "Design and evaluation of a cyber-physical testbed for improving attack resilience of power systems," *IET Cyber-Physical Systems: Theory & Applications*, vol. 6, no. 4, pp. 208–227, 2021.
[26] B. D. Fath, U. M. Scharler, R. E. Ulanowicz, and B. Hannon, "Ecological network analysis: network construction," *Ecological Modelling*, vol. 208, no. 1, pp. 49–55, 2007.
[27] C. E. Shannon, "A mathematical theory of communication," *ACM SIGMOBILE mobile computing and communications review*, vol. 5, no. 1, pp. 3–55, 2001.
[28] A. Bodini and C. Bondavalli, "Towards a sustainable use of water resources: a whole-ecosystem approach using network analysis," *International Journal of Environment and Pollution*, vol. 18, no. 5, pp. 463–485, 2002.
[29] R. E. Ulanowicz, *Growth and development: ecosystems phenomenology*. Springer Science & Business Media, 2012.
[30] A. Layton, "Food webs: realizing biological inspirations for sustainable industrial resource networks," Ph.D. dissertation, Georgia Institute of Technology, 2014.
[31] R. E. Ulanowicz, "An hypothesis on the development of natural communities," *Journal of Theoretical Biology*, vol. 85, no. 2, pp. 223–245, 1980.
[32] R. E. Ulanowicz and J. S. Norden, "Symmetrical overhead in flow networks," *International Journal of Systems Science*, vol. 21, no. 2, pp. 429–437, 1990.
[33] J. Duncan Glover, M. Sarma, and T. Overbye, *Power System Analysis and Design*, 5th ed. Cengage Learning, 2012.
[34] M. Mehrtash and Y. Cao, "A new global solver for transmission expansion planning with ac network model," *IEEE Transactions on Power Systems*, vol. 37, no. 1, pp. 282–293, 2021.
[35] R. Steinberg and W. I. Zangwill, "The prevalence of braess' paradox," *Transportation Science*, vol. 17, no. 3, pp. 301–318, 1983.
[36] S. Blumsack and M. Ilić, "The braess paradox in electric power systems," *Working Paper*, 2006.
[37] B. Schäfer, T. Pesch, D. Manik, J. Gollenstede, G. Lin, H.-P. Beck, D. Witthaut, and M. Timme, "Understanding braess' paradox in power grids," *Nature Communications*, vol. 13, no. 1, pp. 1–9, 2022.
[38] Z. Jin and G. Jin, *Mathematical analysis*. Dalian University of Technology Press Dalian, 2007.
[39] R. D. Zimmerman and C. E. Murillo-Sánchez, "Matpower 6.0 user's manual," *Power Systems Engineering Research Center*, vol. 9, 2016.
[40] K. Davis, "Bio-Inspired Design of Complex Energy Systems," 2021, Texas A&M University, College of Engineering. [Online]. Available: https://katedavis.engr.tamu.edu/projects/bio-inspired-design-of-complex-energy-systems/
[41] A. Wächter and L. T. Biegler, "On the implementation of an interior-point filter line-search algorithm for large-scale nonlinear programming," *Mathematical programming*, vol. 106, no. 1, pp. 25–57, 2006.
[42] O. Kröger, C. Coffrin, H. Hijazi, and H. Nagarajan, "Juniper: An open-source nonlinear branch-and-bound solver in julia," in *International Conference on the Integration of Constraint Programming, Artificial Intelligence, and Operations Research*. Springer, 2018, pp. 377–386.
[43] F. John, V. Stefan, R. Ted, G. S. Haroldo, F. Dan, H. Lou, H. Bill, K. Bjarni, P. Cindy, S. Edwin, L. Miles, W. Jean-Paul, and S. Matthew. (2019, jun) Cbc (coin-or branch and cut) open-source mixed integer programming solver. [Online]. Available: https://github.com/coin-or/Cbc
[44] S. R. Borrett and M. K. Lau, "enar: An r package for ecosystem network analysis," *Methods in Ecology and Evolution*, vol. 5, no. 11, pp. 1206–1213, 2014.
[45] A. B. Birchfield, T. Xu, K. M. Gegner, K. S. Shetye, and T. J. Overbye, "Grid structural characteristics as validation criteria for synthetic networks," *IEEE Transactions on Power Systems*, vol. 32, no. 4, pp. 3258–3265, 2017.
[46] J. W. Busby, K. Baker, M. D. Bazilian, A. Q. Gilbert, E. Grubert, V. Rai, J. D. Rhodes, S. Shidore, C. A. Smith, and M. E. Webber, "Cascading risks: Understanding the 2021 winter blackout in Texas," *Energy Research & Social Science*, vol. 77, p. 102106, 2021.
[47] Y. Koç, M. Warnier, R. E. Kooij, and F. M. Brazier, "An entropy-based metric to quantify the robustness of power grids against cascading failures," *Safety Science*, vol. 59, pp. 126–134, 2013.
[48] B. Bollobás, *Modern graph theory*. Springer Science & Business Media, 2013, vol. 184.
[49] R. Bent, G. L. Toole, and A. Berscheid, "Transmission network expansion planning with complex power flow models," *IEEE Transactions on Power Systems*, vol. 27, no. 2, pp. 904–912, 2011.
[50] J. A. Taylor and F. S. Hover, "Conic ac transmission system planning," *IEEE Transactions on Power Systems*, vol. 28, no. 2, pp. 952–959, 2012.

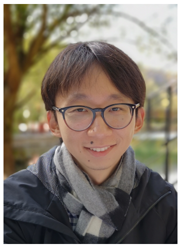

Hao Huang (Member, IEEE) received the B.S. degree in Electrical Engineering (Power System and Its Automation) from Harbin Institute of Technology, Harbin, Heilongjiang Province, China, in 2014, the M.S. degree in Electrical Engineering (Electric Power) from University of Southern California, Los Angeles, CA, USA, in 2016, and the Ph.D. degree in Electrical Engineering at Texas A&M University, College State, TX, USA, in 2022. He is currently a Postdoctoral Research Associate at Princeton University. His research focuses on power system resilience, power system planning and operation, cyber-physical security, and scientific machine learning.

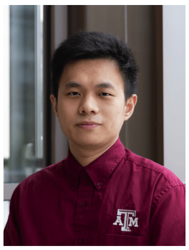

Zeyu Mao (Member, IEEE) received the B.S. degree in Electrical Engineering from Chongqing University, Chongqing, China, in 2015, the M.S. degree in Electrical and Computer Engineering from the University of Illinois at Urbana–Champaign, IL, USA, in 2017 and the Ph.D. degree in Electrical Engineering at Texas A&M University, College State, TX, USA, in 2022. He is currently a Quantitative Trading Analyst at DRW Holdings. His research interests include power system market, power system cyber-physical modeling, data-driven power system control, and sparse matrix ordering.

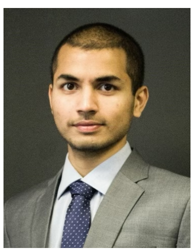

Varuneswara Panyam received the B.S. degree in Mechanical Engineering from Shiv Nadar University, Greater Noida, Uttar Pradesh, India, in 2016, and the M.S. degree in Mechanical Engineering from Texas A&M University, College State, TX, USA, in 2018. He is currently working at Rani Therapeutics.

Astrid Layton received the B.S. degree in Mechanical Engineering from the University of Pittsburgh in Pittsburgh, PA in 2009 and the Ph.D. degree in Mechanical Engineering from Georgia Institute of Technology in Atlanta, Georgia in 2014, respectively. She is currently an Assistant Professor at Texas A&M University in the Mechanical Engineering department. Her research looks at bio-inspired network design problems, focusing on the use of biological ecosystems as inspiration for the design of sustainable and resilient complex human networks and systems.

Katherine R. Davis (Senior Member, IEEE) received the B.S. degree from The University of Texas at Austin, Austin, TX, USA, in 2007, and the M.S. and Ph.D. degrees from the University of Illinois at Urbana–Champaign, Champaign, IL, USA, in 2009 and 2011, respectively, all in electrical engineering. She is currently an Assistant Professor of electrical and computer engineering with Texas A&M University. Her research interests include Operation and Control of Power Systems, Interactions between Computer Networks and Power Networks, Security-oriented Cyber-physical Analysis Techniques, Data-driven and Model-based Coupled Infrastructure Analysis and Simulation.